Chemical Science

Accepted Manuscript

This article can be cited before page numbers have been issued, to do this please use: C. Li, X. Hu, J. Lu, X. Mao, Y. Xiang, Y. Shu and G. Li, *Chem. Sci.*, 2017, DOI: 10.1039/C7SC04663D.

ROYAL SOCIETY OF CHEMISTRY

rsc.li/chemical-science

View Article Online
DOI: 10.1039/C7SC04663D

Journal Name

ARTICLE

Design of DNA nanostructure-based interfacial probes for electrochemical detection of nucleic acid directly in whole blood

Received 00th January 20xx,
Accepted 00th January 20xx

DOI: 10.1039/x0xx00000x

www.rsc.org/

Chao Li[a], Xiaolu Hu[a], Jianyang Lu[a], Xiaoxia Mao[c], Yang Xiang[a,*], Yongqian Shu[b,*], Genxi Li[a,c,*]

Here we report a robust and sensitive DNA nanostructure-based electrochemical (E-nanoDNA) sensor that utilizes tetrahedral DNA nanostructure (TDN) as interfacial probe to detect biomolecules in a single-step procedure. In this study, we have firstly demonstrated that the use of TDNs can significantly suppress the electrochemical background signal compared with the traditional linear DNA probes upon introduction of base mismatch in the edges of TDNs. After further optimization of the two functional strands in the TDNs, quantitative, one-step detection of DNA can be achieved in picomolar range, in less than 10 min, and directly in complex media. Moreover, the baseline drift of this biosensor can be greatly decreased even after several hours in flowing whole blood in vitro, which holds potential to be employed in live animals. Furthermore, through replacing functional strands with aptamers or other DNA elements, this E-nanoDNA sensor can be easily used to probe various analytes, broadening the application range of the proposed sensor.

Introduction

Electrochemical DNA (E-DNA) sensors have provided new opportunities for simple, sensitive, and portable detection of biomolecules relevant to clinical diagnosis and monitoring treatment of diseases.[1] Usually, the signal generation of these sensors originates from the binding-induced changes in the dynamics of the surface immobilized, redox reporter-labeled DNA probe, which affects the flexibility of the probe-target complex, leading to a remarkable change in the redox current.[2, 3] So, these E-DNA sensors are inherently fast, reagentless, portable and cost-effective. However, a crucial issue in E-DNA sensors also exists, i.e., the decreased accessibility of analytes to the probes immobilized on a heterogeneous electrode surface compared with the analyte-probe recognition in homogeneous solution,[4, 5] thus it is easily interfered by endogenous substances (i.e., nucleases, protein, *etc.*), leading to compromised analytical performance. Although many innovative probe designs such as hairpin probes,[6, 7] single or double-stranded probes,[8, 9] triple-stem probes,[10] triblock probe,[11] pseudoknot probes,[12, 13] and antigen-labeled probes[14, 15] have all proven successful at biomolecules (i.e., DNA, proteins, and small molecules, *etc.*) detection, novel strategies that have capacity to improve the recognition abilities of such heterogeneous surface probes are still required.[16] Moreover, recently, new challenge has been proposed to E-DNA sensors, which is expected to be used to realize real-time analysis of analytes in living animals,[17, 18] while conventional probes may suffer poor robustness in the complex matrix (i.e., whole blood), impairing the analytical performance of E-DNA sensors. Therefore, the development of novel electrochemical probes for construction of E-DNA sensors which may meet the increasing requirement of bioanalysis is highly desirable.

As a matter of fact, since the orientation and the distribution of traditional linear DNA probes on the electrode surface are difficult to control, Fan and co-workers have reported a novel electrochemical sensor based on 3D nanostructure DNA probes.[19-21] In their design, a tetrahedral DNA nanostructure (TDN) containing a capture probe at one vertex and three thiol groups at the other vertices is designed and immobilized on the gold electrode surface. Thanks to the rigid and arrayed DNA nanostructures, greatly improved sensitivity is achieved compared to conventional E-DNA sensors based on single-stranded DNA (ssDNA) considering the entanglement between the probes and the localized aggregation of probes. Nevertheless, since the signal generation of this sensor necessarily depends on the formation of sandwich structure, namely "DNA tetrahedron/target molecule/signal probe/enzyme", it requires multiple incubation and washing steps and the addition of exogenous biotin-labeled DNA strand and streptavidin-labeled enzyme, making the whole assay expensive, laborious and time-consuming, which impedes its use in point-of-care testing (POCT).

[a] State Key Laboratory of Pharmaceutical Biotechnology and Collaborative Innovation Center of Chemistry for Life Sciences, Department of Biochemistry, Nanjing University, Nanjing 210093, P. R. China. Email: xiangy@nju.edu.cn (Y. Xiang), yongqianshu531@163.com (Y. Shu), genxililab@nju.edu.cn (G. Li); Tel: +86-25-83593596.
[b] Department of Oncology, the First Affiliated Hospital of Nanjing Medical University, Nanjing 210029, P. R. China
[c] Laboratory of Biosensing Technology, School of Life Sciences, Shanghai University, Shanghai, 200444, China

† Footnotes relating to the title and/or authors should appear here.
Electronic Supplementary Information (ESI) available: [details of any supplementary information available should be included here]. See DOI: 10.1039/x0xx00000x

View Article Online
DOI: 10.1039/C7SC04663D

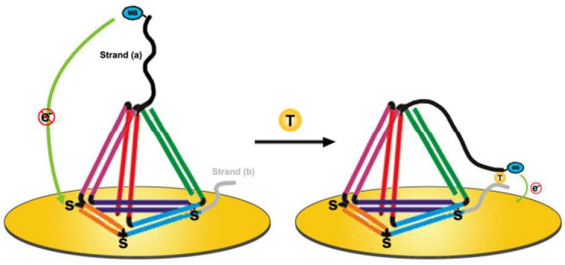

Scheme 1. E-nanoDNA sensor contains an electrode-bound, redox-reporter modified tetrahedral DNA nanostructure containing two functional strands (black and grey) that undergoes a target binding-induced conformational change on the electrode surface. This conformational change pulls the reporter (methylene blue, MB) close to the electrode surface (yellow disk), thereby producing a target-dependent change in current when the sensor is interrogated by square wave voltammetry.

Herein, we present a novel DNA nanostructure-based electrochemical (E-nanoDNA) sensor that overcomes the drawbacks of the above-mentioned two kinds of sensors. Building upon the pioneering works by Plaxco group and Fan group, we have added the DNA nanostructure to the E-DNA sensor. To do so, we have designed a TDN with two additional stands appended to the two vertexes (Scheme 1, left). The top one functions as capture strand (a) and the other one at the bottom acts as assistant strand (b). This allows us to flexibly add recognition elements that specifically bind the analyte of interest through choosing appropriate DNA elements (i.e., DNA, aptamer, and DNAzyme, *etc*.) and covalently modifying electrochemical species. The functional part of strand (a) has a relatively long sequence [(9 nucleotides (nt)] and the melting temperature of the strand (a): target duplex is 41.2 °C. Stand (b) has a relatively short sequence (6 nt) and the melting temperature of the strand (b): target duplex is less than 1 °C (1 μM DNA in 10 mM sodium phosphate, 0.5 M NaCl, 1.5 mM $MgCl_2$ pH 7.4 buffer). By using three thiolated ssDNA as anchoring legs, thiol modifications on three vertices of the "bottom" face of TDN are designed as anchoring units for the immobilization on electrode surface. In the absence of target, the strand (a) sequesters the methylene blue (MB) molecule from the electrode surface due to the strong steric effect induced by large and rigid DNA nanostructures, producing a feeble MB redox current. Upon target binding, the observed MB redox current increases significantly. The proposed sensor underlying this signaling is as follows. Target is firstly captured by strand (a) through DNA hybridization. Then, short stand (b) binds with strand (a)/target complex to form an intact structure (T_m = 63.3 °C) and provides traction to pull down the strand (a), increasing the chance of the MB to collide with electrode surface and facilitating the electron transfer (Scheme 1, right). This E-nanoDNA sensor has combined the advantages of traditional E-DNA sensors and TDN-based electrochemical sensors. First, it can more efficiently capture analyte and suppress background current, indicating better analytical performance. Second, DNA nanostructure is more stable and insensitive to biofouling than linear DNA probes in the complex matrices, promoting the reproducibility of the sensor. Third, the testing can be achieved by only one-step incubation without requiring additional reagents and washing steps, greatly reducing the operating difficulty.

Results and discussion

To improve the analytical performance of E-nanoDNA sensor, two different strategies can be employed: lowered background signal and amplified detection. In the first case, considering previous E-DNA sensors have widely employed a floppy or relatively rigid DNA probe (i.e., ssDNA or dsDNA), thus large electrochemical signals come from dynamic collision between the electrode and the redox moiety without addition of target, attenuating the signal gain. The hypothesis is that increasing the size of DNA probe can efficiently reduce the collision chance between the electrode and the redox moiety, thereby reducing background current. Therefore, a series of DNA probes with different sizes, ssDNA25, TDN10, TDN20, and TDN30 (ssDNA has 25 nt and each edge of the TDN contains 10, 20, or 30 base pairs, respectively), have been employed to test the background signal. All used sequences are rationally designed with the aid of structural prediction tools (NUPACK software) to avoid undesired secondary structures appearing at the edges. Because each base pair is separated by 0.34 nm in a double helix, the edge length of these TDNs is 3.4, 6.8, and 10.2 nm, respectively. Since the persistence length of ssDNA is about 1 nm, we can estimate the height of these probes on the electrode surface to be 2, 3.8, 6.5, and 9.3 nm (a six-carbon spacer forms a layer of ~ 1 nm). TDNs are assembled with four different ssDNA through a facile annealing process. Gel electrophoresis, atomic force microscopy (AFM), and dynamic scatting light (DLS) results confirm the successful formation of the DNA tetrahedron (Figure S1). Figure 1A compares the background signals of the sensor modified with ssDNA25, TDN10, TDN20, and TDN30. The surface coverage of these probes, determined by quartz crystal microbalance (Figure S2), is maintained within the range of (2.5 ± 0.4) × 10^{12} molecules/cm^{-2} throughout this study, thus the nanospacing between the DNA probes is ~5.0 nm, which is advantageous to capture analyte. The electrochemical behavior is investigated by square wave voltammetry (SWV), which allows highly sensitive detection of very low concentrations of a redox probe. Compared to background peak current of 1887 nA with ssDNA25, as hypothesized, it is indeed possible to reduce the background signal by 2.1-fold using TDN10. This result demonstrates that large framework of the tetrahedron indeed prevents direct collision between MB and the electrode surface. However, the background peak currents don't obviously attenuate using TDN20 and TDN30, though they have larger spatial structures. This is probably owing to the fact that MB molecules can directly pass the electron through DNA backbone, leading to a large background signal.

To find out the real reasons for above results, our next attempt is to introduce one-base-pair mismatch in the edge of

View Article Online
DOI: 10.1039/C7SC04663D

the TDN20 and TDN30 at the bottom site to block charge passing through the DNA double helices, since MB transporting

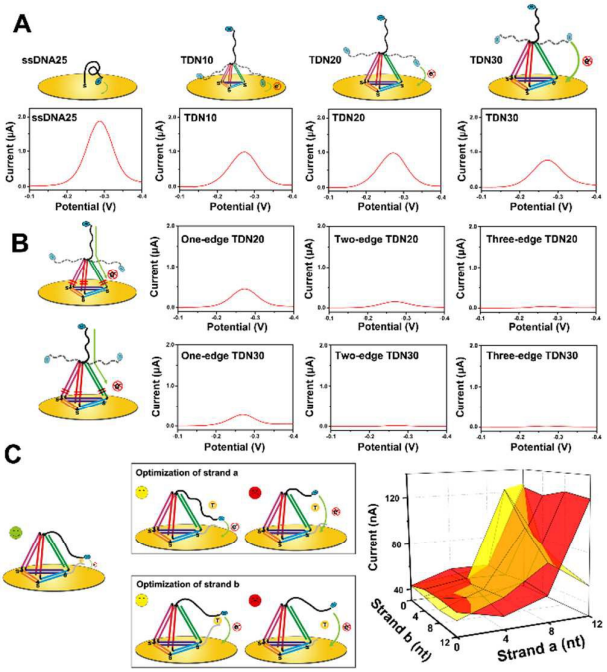

Figure 1. Optimization of E-nanoDNA sensor through reducing background signals and promoting positive signals in the presence of analyte. (A) Background signals obtained from sensors modified with different probes, ssDNA25, TDN10, TDN20 and TDN30. (B) Background signals obtained from sensors modified with TDNs containing a different number of one-base mismatches. (C) Optimization of the spacer lengths of strand (a) and strand (b) for better analytical performance in the absence (red) or presence (yellow) of target (1 nM).

electrons are very sensitive to perturbation of π-stacking in the duplex (Figure 1B, left).[22, 23] As hypothesized, the introduction of one-base-pair mismatch in the one edge of TDN20 and TDN30 successfully blocks the electron transfer of MB via stacked nucleobases, resulting in the decrease of background peak current from 764 nA and 695 nA down to 387 nA and 234 nA, respectively (Figure 1B). Furthermore, when one-base-pair mismatch is respectively introduced into the two or three edges of TDN20 and TDN30, the background signal reduces close to baseline. Considering the large TDN30 requires synthesis of a long DNA sequence and the synthesis of larger TDN (e.g., TDN40) requires more complex method, so a TDN20 containing three one-base-pair mismatches is chosen as the electrochemical probe.

Next, in order to amplify positive signal, MB head, in principle, needs to be pulled as close as possible to the underlying electrode, where the electron could be transferred by tunneling between the redox label and the gold electrode. So, the spacer length of strand (a) and strand (b) should be carefully optimized. When the strands are too short, the formation of intact "strand (a)/strand (b)/target" complex is prohibited, failing to generate any detective signals. In the case of long spacer of strand (a) (i.e., 12 nt), a large background signal is observed, which indicates that strand (a) may directly interact with electrode surface (Figure 1C, upper).

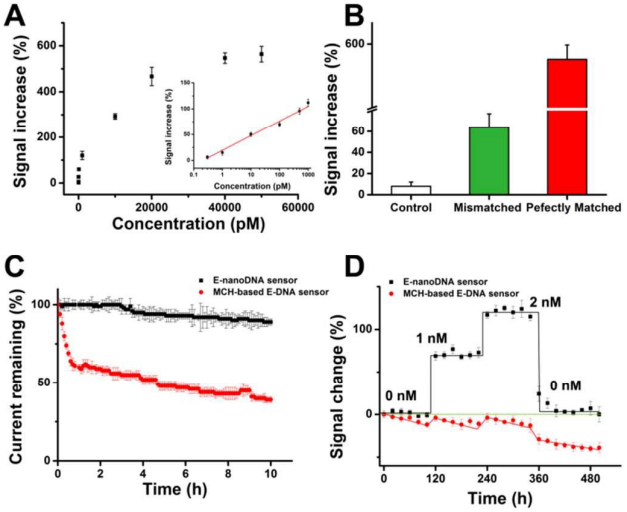

Figure 2. The application of E-nanoDNA sensor for DNA detection. (A) The dynamic range of the E-nanoDNA sensor covers target concentrations from 300 fM to 50 nM. Inset: detection of DNA in the low concentration range. (B) Comparison of electrochemical signals obtained by the E-nanoDNA sensor with a control strand (random strand, 50 nM), one-base mismatched strand (50 nM), and a perfectly matched probe (50 nM). (C) When challenged in flowing whole blood (no target), E-nanoDNA sensors (black) exhibit less than 11% current drift over 10 h, while the original signal of conventional MCH-based E-DNA sensors (red) loses around 61%. (D) The improved drift performance of the E-nanoDNA sensors allows real-time analysis in whole blood. Shown are data recorded in flowing whole blood samples in vitro spiked with target DNA at different time points. Error bars show the standard deviation of at least three independently matched electrodes to record this data set.

However, the sensor can also response to the target molecules and obtain reduced current, which indicates that the sensor becomes to be "signal-off" model. As for spacer of strand (b), upon increasing the length of spacer (> 4 bp), it also leads to reduced signaling current in the presence of analyte (Figure 1C, bottom), indicating that the formed complex is pulled away from the electrode surface, decreasing the interaction chance of MB with electrode surface. Therefore, the spacer length of strand (a) and strand (b) is selected as 8 nt and 4 nt, respectively.

After determination of the DNA nanostructure, sensor performance has been first evaluated by detection of DNA molecule. We observe that the new E-nanoDNA sensor responds rapidly (~ 8 min, Figure S3) and robustly (standard deviation across three electrodes < 5%) to its target. The signaling current increases significantly as we titrate the sensor with increasing amounts of target DNA (Figure 2A). The detection limit of the current sensor is 300 fM (> 3 SD, standard deviation), and the useful dynamic range spans four orders of magnitude (Figure 2A, inset). This sensitivity is superior to many developed E-DNA sensors or DNA nanostructure-based electrochemical sensors (Table S2). In

View Article Online
DOI: 10.1039/C7SC04663D

contrast, control experiments reveal that the addition of a one-base mismatched target at a concentration of 50 nM

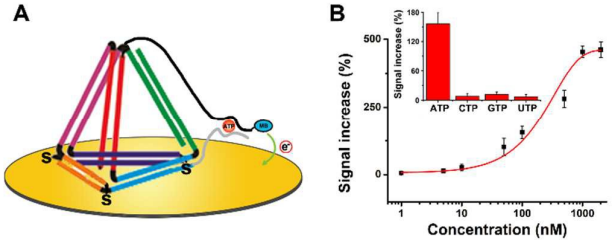

Figure 3. The application of EA-nanoDNA sensor for ATP detection. (A) EA-nanoDNA sensor-based ATP detection scheme. b) Quantitative results for detecting varying concentrations of ATP. Inset: Selectivity study using CTP, GTP, and UTP as control molecules, [ATP, CTP, GTP, UTP] = 100 nM.

(which would be a saturating target concentration for the perfect match) only produces ~64% signal change (Figure 2B). The E-nanoDNA sensor is highly resistant to complex sample (i.e., serum), with feeble alteration of the background noise and nearly the same hybridization signal for the 1 nM target, in the presence of 100% serum (Figure S4).

More importantly, Plaxco et al. have demonstrated that traditional 6-mercapto-1-hexanol (MCH)-based E-DNA sensors suffer from severe drift when employed in flowing whole blood,[24] which greatly limits their application in continuous, real-time, and chip-based measurements. Due to the robustness and antifouling ability of DNA nanostructure, we are motivated to investigate whether E-nanoDNA sensor can eliminate the drift seen in the flowing sample without intricate correction algorithms, thereby resulting in stable analytical performance under hours of successive operation. Figure 2C demonstrates that the E-nanoDNA sensor exhibits excellent baseline stability over the course of 10 h in flowing whole blood, while the signal from MCH-based sensor reduced to ~39%. Under these same conditions, the E-nanoDNA sensor responds quantitatively to their target in flowing whole blood and return quantitatively to their original baseline when the target is removed (Figure 2D), achieving nanomolar precision in the measurement of DNA; however, the MCH-based sensor shows evident drift in both the presence and absence of target.

Subsequently, we believe that this new E-nanoDNA sensor may provide a versatile platform for the analysis of a wide range of biomolecules by taking advantage of aptamers. To assemble the aptamer-based E-nanoDNA (EA-nanoDNA) sensor, we have replaced the DNA probe with an anti-adenosine triphosphate (ATP) aptamer sequence that is divided into two different fragments, and assembled the aptasensor on gold surfaces. In the absence of ATP, the split aptamer strands don't interact with each other. Upon introduction of ATP, the two fragments are induced to form strong aptamer-target complex, generating a large signaling current. As shown in Figure 3, this EA-nanoDNA sensor shows excellent sensitivity toward ATP, with a remarkable detection limit of 5 nM (Figure 3A), which is lower than the ssDNA aptamer-based sensors.[25, 26] The specificity has been further tested in the presence of possible interference, such as CTP, GTP, and UTP. The alternation in electrochemical response induced by the non-specific binding between the ATP analogues above is much lower than that of the response induced by the specific binding of ATP (Figure 3B, inset), demonstrating the excellent selectivity of EA-nanoDNA sensor. The main text of the article should appear here with headings as appropriate.

Conclusions

In summary, we have constructed a novel DNA nanostructure-based E-DNA sensor for direct detection of biomolecules. In this system, the two additional strands extended from the two vertexes of TDN folds around the analyte bringing the MB molecule in close proximity to the electrode surface affording an electrochemical response. Unlike prior reagentless electrochemical E-DNA sensor based on ssDNA or DNA hairpins with weak rigidity, this approach provides a more robust platform with improved analytical performance. Compared with previous DNA tetrahedron-based electrochemical sensors using enzyme-turnover as signal generation, this method requires no expensive, additional reagent and multiple incubation and washing steps, thus greatly simplifying the operation procedures, which is highly desirable for POC diagnostic sensors. However, currently, this type of E-sensor still relies on the 1:1 binding model and one target molecule only generates one signal event, so the sensitivity is inferior to the enzyme-assistant ones. Therefore, our next work will focus on the optimization of electrode surface and attempt to employ amplification elements into the proposed sensor. We also believe that other DNA nanostructures, such as DNA box, DNA nanosheet, DNA prism, *etc.*, can also be used as electrochemical probes after appropriate design, which may further improve the performance of the proposed biosensor. All together, these results are the first example of the application of DNA nanostructure as bifunctional probes for the electrochemical detection of biomolecules of interest and can pave the way for the design of other innovative analytical systems.

Experimental

Materials and Reagents

DNA oligonucleotides were synthesized and purified by Sangon Biotechnology Inc. (Shanghai, China). 6-Mercaptohexanol (MCH), tris(2-carboxyethyl)phosphine hydrochloride (TCEP), adenosine triphosphate (ATP) and hexaammineruthenium(III) chloride (RuHex) were purchased from Sigma. Foetal bovine serum (FBS) was purchased from Life Technologies (Gibco). Blood was collected from lab's volunteers. All other chemicals were of analytical grade and were used without further purification. All solutions were prepared with Milli-Q water from a Millipore system.

The buffers employed were as follows: the DNA tetrahedron preparation and immobilization buffer was 10 mM Tris-HCl, 10

View Article Online
DOI: 10.1039/C7SC04663D

mM $MgCl_2$, pH 7.4. The electrodes were washed in 0.2 M PBS. The hybridization reactions were performed in 10 mM Tris-HCl, 0.5 M NaCl, 1.5 mM $MgCl_2$, pH 7.4. Electrochemical detection for methylene blue (MB) was performed in 20 mM PBS, 0.5 M NaCl, pH 7.4.

Preparation of DNA tetrahedron

Equal quantities of four strands for the formation of the tetrahedrons were mixed in preparation buffer at a final concentration of 1 μM and then heated to 95 °C for 10 min and immediately cooled to 4 °C. The characterization of synthesized DNA tetrahedron is used for atomic force microscope (AFM) and dynamic light scatting (DLS) study.

Preparation of the modified gold electrodes and surface area determination

Gold electrodes (1 mm in diameter) were polished on microcloth with 0.3 μm and 0.05 μm γ-alumina. The polished electrodes were then sonicated in ethanol and pure water for 2 min each. Lastly, the electrodes were electrochemically in 0.5 M H_2SO_4 by scanning the potential between the oxidation and reduction of gold, -0.35 V and 1.5 V, respectively. All electrochemical measurements were carried out with a CHI 660D electrochemical workstation (CH Instruments Inc., Austin). A three-electrode configuration was employed in all experiments and involved a gold working electrode, a platinum wire counter electrode and a saturated calomel reference electrode (SCE).

Electrode modification

A 10 μL volume of 1 μM tetrahedron probes in immobilization buffer (containing 5 mM TCEP) was dropped to the surface of the cleaned gold electrodes and incubated for 2 h at room temperature. The modification for single-stranded DNA (ssDNA) was the same as that for the tetrahedrons, and the concentration was also 1 μM. However, for the modification of ssDNA, the modified electrodes were then exposed to a 1 mM MCH solution at room temperature for 1 hour to replace non-specific interactions and form a self-assembled monolayer (SAM). Between each step, the electrode was rinsed and dried with N_2. Then, the modified electrodes were incubated with different concentration of target probe at 37 °C for 10 min.

Target detection

For DNA and ATP assays, the modified electrodes were incubated in target solution of various concentrations for 10 min at 37 °C. The electrodes were then extensively rinsed with washing buffer and subjected to electrochemical measurements.

Electrochemical measurements

Square wave voltammetry (SWV) was performed using a potential window of -0.1 to -0.4 V (versus SCE), 1 mV potential step, 50 mV amplitude and 20 Hz frequency.

Real-Time Detection of DNA in Continuously Flowing blood

For real-time DNA detection, samples of blood prepared in syringes and doped with different concentrations of DNA. The syringe was connected to a closed-loop system equipped with flow-cell screen-printed electrodes (DropSens, Spain). All the experiments were conducted in a closed-loop system with a continuous flow of whole blood (1 mL/s) using a circulator pump to mimic circulation in the vasculature. At each concentration, SWV measurements were performed every 15 s scanning from -0.15 to -0.55 V, and the peak reduction current is recorded using a computer controlled data acquisition system. The sensors after target response experiments were regenerated by washing with fresh blood.

Live subject statement

All blood tests described in the project were performed in the laboratory of Professor of Genxi Li, as approved under the Nanjing Drum Tower Hospital of Nanjing University Medical School Ethics Committee.

Conflicts of interest

There are no conflicts to declare.

Acknowledgements

This work is supported by the National Natural Science Foundation of China (Grant Nos. 21235003, 81672570, J1210026), the Science Foundation of Jiangsu Province, China (Grant No. BM2015023), and Fundamental Research Funds for the Central Universities in China (Grant No. 021414380001).

References

1. J. Wang, *Biosens. Bioelectron.*, 2006, **21**, 1887-1892.
2. A. A. Lubin and K. W. Plaxco, *Acc. Chem. Res.*, 2010, **43**, 496-505.
3. K. Hsieh, B. S. Ferguson, M. Eisenstein, K. W. Plaxco and H. T. Soh, *Acc. Chem. Res.*, 2015, **48**, 911-920.
4. H. Pei, X. Zuo, D. Zhu, Q. Huang and C. Fan, *Acc. Chem. Res.*, 2013, **47**, 550-559.
5. H. Kimura-Suda, D. Y. Petrovykh, M. J. Tarlov and L. J. Whitman, *J. Am. Chem. Soc.*, 2003, **125**, 9014-9015.
6. C. H. Fan, K. W. Plaxco and A. J. Heeger, *P. Natl. Acad. Sci. USA*, 2003, **100**, 9134-9137.
7. Z.-g. Yu and R. Y. Lai, *Chem. Commun.*, 2012, **48**, 10523-10525.
8. Y. Wu and R. Y. Lai, *Anal. Chem.*, 2014, **86**, 8888-8895.
9. C. Li, X. Li, L. Wei, M. Liu, Y. Chen and G. Li, *Chem. Sci.*, 2015, **6**, 4311-4317.
10. Y. Xiao, X. Lou, T. Uzawa, K. J. Plakos, K. W. Plaxco and H. T. Soh, *J. Am. Chem. Soc.*, 2009, **131**, 15311-15316.
11. C. E. Immoos, S. J. Lee and M. W. Grinstaff, *J. Am. Chem. Soc.*, 2004, **126**, 10814-10815.
12. Y. Xiao, X. Qu, K. W. Plaxco and A. J. Heeger, *J. Am. Chem. Soc.*, 2007, **129**, 11896-11897.
13. K. J. Cash, A. J. Heeger, K. W. Plaxco and Y. Xiao, *Anal. Chem.*, 2008, **81**, 656-661.
14. K. J. Cash, F. Ricci and K. W. Plaxco, *J. Am. Chem. Soc.*, 2009, **131**, 6955-6957
15. C. Li, Y. Tao, Y. Yang, Y. Xiang and G. Li, *Anal. Chem.*, 2017, **89**, 5003-5007.
16. C. Li, D. Wu, X. Hu, Y. Xiang, Y. Shu and G. Li, *Anal. Chem.*, 2016, **88**, 7583-7590.
17. H. Li, P. Dauphin-Ducharme, N. Arroyo-Curras, C. H. Tran, P. A. Vieira, S. Li, C. Shin, J. Somerson, T. E. Kippin and K. W. Plaxco, *Angew. Chem. Int. Ed.*, 2017, **56**, 7492-7495.

View Article Online
DOI: 10.1039/C7SC04663D

18. N. Arroyo-Currás, J. Somerson, P. A. Vieira, K. L. Ploense, T. E. Kippin and K. W. Plaxco, *P. Natl. Acad. Sci. USA*, 2017, 201613458.
19. H. Pei, N. Lu, Y. Wen, S. Song, Y. Liu, H. Yan and C. Fan, *Adv. Mater.*, 2010, **22**, 4754-4758.
20. M. Lin, P. Song, G. Zhou, X. Zuo, A. Aldalbahi, X. Lou, J. Shi and C. Fan, *Nat. Protoc.*, 2016, **11**, 1244-1263.
21. M. Lin, J. Wang, G. Zhou, J. Wang, N. Wu, J. Lu, J. Gao, X. Chen, J. Shi, X. Zuo and C. Fan, *Angew. Chem. Int. Ed.*, 2015, **54**, 2151-2155.
22. J. D. Slinker, N. B. Muren, S. E. Renfrew and J. K. Barton, *Nat. Chem.*, 2011, **3**, 228-233.
23. N. Lu, H. Pei, Z. L. Ge, C. R. Simmons, H. Yan and C. H. Fan, *J. Am. Chem. Soc.*, 2012, **134**, 13148-13151.
24. H. Li, N. Arroyo-Curras, D. Kang, F. Ricci and K. W. Plaxco, *J. Am. Chem. Soc.*, 2016, **138**, 15809-15812.
25. M. Zayats, Y. Huang, R. Gill, C.-a. Ma and I. Willner, *J. Am. Chem. Soc.*, 2006, **128**, 13666-13667.
26. X. Zuo, S. Song, J. Zhang, D. Pan, L. Wang and C. Fan, *J. Am. Chem. Soc.*, 2007, **129**, 1042-1043.

View Article Online
DOI: 10.1039/C7SC04663D

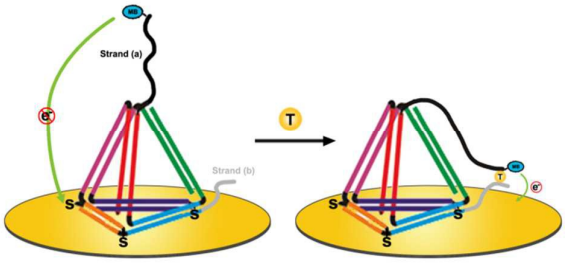

A novel DNA nanostructure-based electrochemical (E-nanoDNA) sensor is proposed for one-step and reagentless detection of biomolecules in flowing sample.